Study on Taylor Vortex Formation in a Liquid Gap with Significant Bounary Effects

Rensheng Deng[1, 2], Make Yechyn[3], Chi-Hwa Wang[2, 3] and Kenneth A. Smith[1, 2]

[1] Department of Chemical Engineering, Massachusetts Institute of Technology, Cambridge, MA 02139

[2] Singapore-MIT Alliance, 4 Engineering Drive 3, Singapore 117576

[3] Department of Chemical & Biomolecular Engineering, National University of Singapore, 4 Engineering Drive 4, Singapore, 117576

Prepared for presentation at the 2005 AIChE Annual Meeting

Cincinnati, OH, October 30 – November 4.

September, 2005

Unpublished

Abstract

Here we present a study on the Taylor vortices formed in a mineral oil between a rotating inner cylinder and a stationary outer cylinder. The apparatus is featured with a wide gap (radius ratio is 0.613) and a short liquid column (aspect ratio is 5.17). Particle image velocimetry (PIV) system was adopted to determine the position, shape and velocity distribution of the vortices. The experimental results show that the transition to wavy vortex flow occurs at a very high Reynolds number than in an infinitely long column, while an asymmetric feature was observed in the widths of the inflow and outflow regions. The simulation results from computational fluid dynamics (CFD) can satisfactorily reproduce the vortex structures, and the calculated maximum axial velocity agrees well with the PIV measurements. The effects of both the top and bottom ends on the vortex flow were also examined.

1 Introduction

Taylor vortex flow is a classical topic in fluid mechanics and it has found increasing application to processes such as reaction, filtration and extraction. Usually, Taylor vortices are studied in devices that have narrow gaps ($d=R_o-R_i$, where R_o and R_i are the radii of the outer and inner cylinders, respectively) and high aspect ratios ($\Gamma=H/d$, where H is the length of the liquid column) in order to avoid end effects. However, it is also known that Taylor vortices formed in short, wide gap devices exhibit novel features. These include, for example, a much higher critical Reynolds number for transition from Taylor vortex flow to wavy vortex flow than in the case of infinitely long cylinders (Cole, 1976; Edwards, Beane and Varma, 1991), and the appearance of “anomalous” vortices in those sudden start experiments (Benjamin, 1978; Koga and Koschmieder, 1989; Bielek and Koschmieder, 1990). A quantitative characterization of the flow in short liquid columns will help to provide a better understanding of the above features.

As a powerful, non-intrusive method for flow diagnosis, particle image velocimetry (PIV) is widely used in the study of fluid mechanics in recent years. However, only several limited PIV measurements have been made in the velocity fields of non-wavy Taylor vortex flow. Wereley and Lueptow (1998) experimentally determined characters of both non-wavy and wavy vortices (Γ=47.7) although their major efforts were put on the latter. Painter and Behringer (1998) examined the effects of spatial disorder on the transition to Taylor vortex flow (Γ=33.4). Wereley, Akonur and Lueptow (2002) measured the particle-fluid velocities in rotating filtration of a suspension (Γ=45-48) using both PIV and PTV (particle tracking velocimetry). In the study of liquid flow between an rotating inner cylinder having a periodically varying radius along the axial direction and an outer stationary cylinder with a constant radius, Drozdov, Rafique and Skali-Lami (2004) measured the axial and radial velocities with the help of PIV (Γ>20). According to our knowledge, the sole work concerning PIV application on a liquid column with Γ<10 was presented by Smieszek and Egbers (2005), although no quantitative velocity data were reported in their paper.

The significant progress in computational capacity and algorithm (for example, finite element method) makes it possible to apply computational fluid dynamics (CFD) simulation

to the study of complex flows in various processes. For example, the commercial CFD software package, Fluent, was employed by researchers to study the single-phase (Wang et al., 2005; Wang, Vigil and Fox, 2005; Marchisio, Barresi and Fox, 2001; Marchisio and Barresi, 2003; Dutta and Ray, 2004) or two-phase Taylor-Couette flow systems (Zhu and Vigil, 2001; Baier and Graham, 2000; Baier, Graham and Lightfoot, 2000). The simulation results for both the laminar and turbulent flows were reported to be satisfactory, although again a specific investigation on the short-column problem is not available. Indeed, in comparison of the analytical solution methods usually accompanied by lots of assumptions, CFD is especially effective in examining the strong boundary effects corresponding to the Taylor vortex within a liquid column of finite length.

In this paper, we present a study on the Taylor vortex formation in a wide liquid gap within a short column. Both PIV measurements and CFD calculations are used to characterize the flow field in the presence of significant boundary effects.

2 Methodology

2.1 Experimental apparatus and procedure

A schematic diagram of the experimental apparatus is shown in Figure 1. A Newtonian mineral oil (with a density ρ of 0.86 g/cm^3 and a viscosity μ of 29.7cp) is adopted as the working liquid within the annulus between a stationary outer cylinder (R_o=30mm, L=200mm) and a rotating inner cylinder (R_i=18.4mm, H=60mm). This gives a gap width (d) of 11.6 mm, a radius ratio $\eta=R_i/R_o$ of 0.613 and an aspect ratio Γ of 5.17. The inner cylinder is made of stainless steel and is propelled by a motor through a shaft of 6mm in diameter. The rotation speed Ω of the motor can be set continuously between 0 to 800rpm by a computer, and the high viscosity of the mineral oil ensures laminar flow in the whole speed range. The outer cylinder is made of Plexiglas and immersed in a Plexiglas square box (70mmX70mmX180mm) filled with the mineral oil mentioned above to eliminate the optical distortion. Except in the study of top and bottom effects, the distance between the bottom of inner cylinder and the bottom of outer cylinder (H_B) is always set at 72mm, and the distance between the top of the inner cylinder and the liquid surface (H_T) is set at 6mm. The controlling parameter is Reynolds number

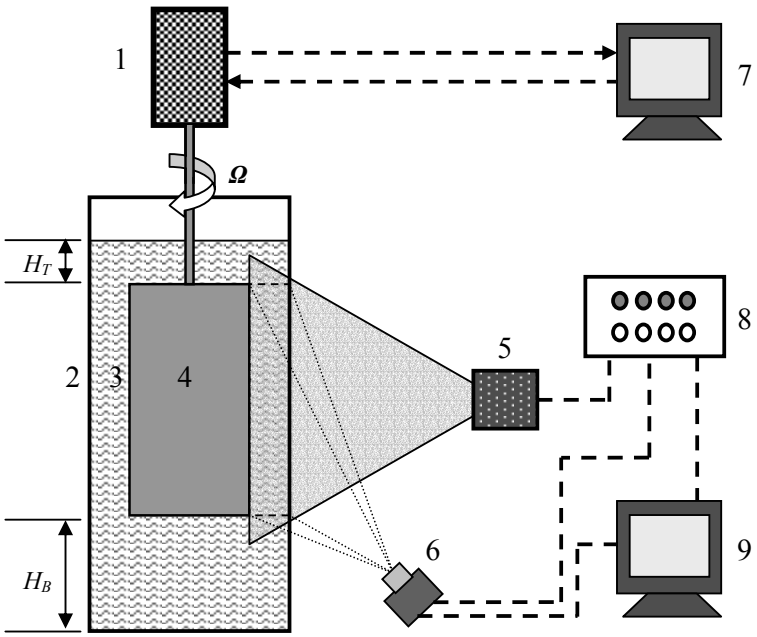

Figure 1: Schematic diagram of the experimental set-up (1) Motor (2) Outer cylinder (3) Working liquid (4) Inner cylinder (5) Laser generator (6) Camera (7) Computer for motor control (8) Synchronizer (9) Computer for PIV system.

($Re=\Omega d R_i/\mu$), which can be up to 519 for the present apparatus.

A PowerView 2-D PIV system from TSI Company (Shoreview, Minnesota, USA) is adopted to monitor the liquid flow, by which the position, shape and velocity distribution of Taylor vortices can be determined. The laser lightsheet generated by the Laser Pulse^{TM} Solo Mini Dual Nd:YAG laser is introduced from the sidewall to lighten the annulus. Silver coated hallow glass spheres of average diameter size and density of 16 μm and 1.6 g/cm^3 respectively are added as tracer particles into the fluid system. These tracer particles show an excellent reflection to the laser light and follow the liquid flow well. Images of the tracer particles are captured by a PowerView^{TM} 4M 2Kx2K camera at the direction perpendicular to the lightsheet. Two photos are taken within a short time interval (dT ranges from 200 to 2000μs) and the image data are then sent to the computer for processing. A LaserPulse^{TM} Computer Controlled Synchronizer is adopted to coordinate the operation of the whole PIV system. The image data are analyzed in the Insight^{TM} Parallel Processing Ultra PIV software using a cross-correlation algorithm to generate the velocity vectors.

Before the PIV measurements were carried out, a calibration step was conducted in order to transfer displacement from the unit of pixel into millimeter. This was done by photographing an object of known size at the site where the laser lightsheet passes by and comparing the pixel distance in the image and the corresponding real length of the object. Because the time scale is obtained directly from the synchronizer, the actual velocity can then be determined.

It is well know that “historic effect” plays an important role in the Taylor vortex formation. Different from the usual “sudden start” and “quasisteady” experiments, the inner cylinder in our experiments was run at the maximum rotational speed of 800.4 rpm for 1 min and then suddenly decelerated to the desired rotation speed. This is to ensure rich tracer particles floating in the liquid such that the highest resolution of velocity vectors can be achieved. After comparing the velocity fields obtained at different moments after the “sudden deceleration”, a waiting time of 12 minutes was selected to wait for the flow to reach the steady state. The repeating tests show that the above method can produce satisfactory velocity data of the steady state corresponding to a certain rotation speed.

2.2 Numerical method

In this study, Fluent 6.1 is adopted to simulate the Taylor vortex flow. The calculation domain is configured in Gambit 2.1, with all the structures of the apparatus being identical to those used in experiments. The flow is considered to be axisymmetric, and the walls of the inner and outer cylinders were no-slip. However, the shear stress at the liquid surface is set to be zero, while experimentally that surface is the interface between gas and liquid. The simulation followed the same “sudden deceleration” procedure as adopted in the experiments, in an effort to model any hysteresis effects that might be present.

3 Results and discussion

3.1 Vortex structure in a short column

It is found that a Taylor vortex first appears at a critical Reynolds number Re_c of 62 and persists to at least a Reynolds number of 519 in the present system. The observed critical Reynolds number is fully consistent with the prediction of Yim *et al*. (1998) for this radius ratio. It should also be noted that the data show no sign of wavy vortices and this is consistent with the predictions of Edwards *et al*. (1991) for low aspect ratio devices. Compared to the devices with a large aspect ratio (for instance, Wereley and Lueptow [1998] reported the critical Reynolds number of 102 at the onset to Taylor vortex and 131 at the onset to wavy vortex corresponding to Γ=47.7), the short-column apparatus provides a much wider range of Reynolds number for non-wavy Taylor vortex flow.

Figure 2a shows a typical chart of velocity vectors obtained from PIV measurements. It can be seen that there are three pairs of vortices in the annulus along the vertical direction. The vortex centers are displaced towards the outer cylinder in the Taylor vortex flow regime, which agrees with the observation of Smieszek and Egbers (2005).

For a liquid column with fixed ends, it is not difficult to predict the flow direction of the end vortices as a result of the Ekman pumping. For end walls rotating with the inner cylinder, centrifugal viscous pumping causes an outflow at the end walls. For end walls fixed to the outer cylinder, the imbalanced pressure gradient and centrifugal forces result in an inflow at the end walls (Czarny, 2002). In the present case, although the bottom of the outer cylinder is not directly fixed at the end of the narrow gap, a similar analysis on the force balance shows that there is an inflow in the liquid layer below the bottom of the inner cylinder. Thus, a clockwise vortex flow shown in Figure 2 is always observed in our experiments. However, the liquid has a free surface on the top, which makes it difficult to predict the vortex direction there. This can be seen more clearly in the study of top effects to be described later.

Another feature shown in Figure 2a is that the vortex is not uniformly

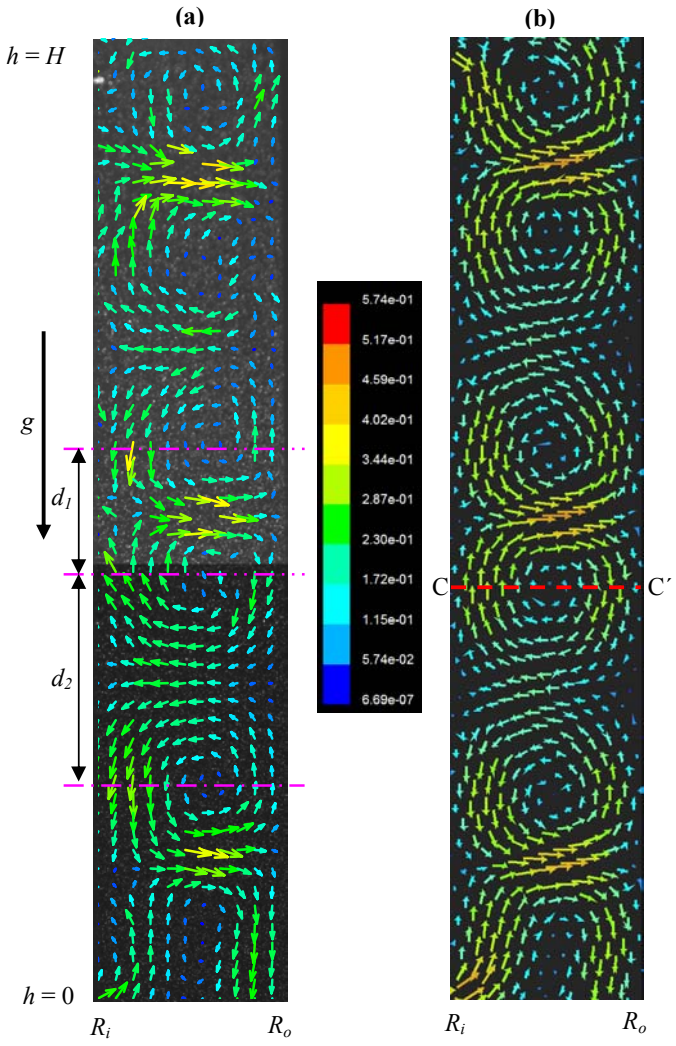

Figure 2: Velocity field (a) from PIV measurement and (b) from Fluent simulation. *Re*=194. Here *g* is the gravitational acceleration, h is the vertical position. The color bar between (a) and (b) shows the common velocity scale (m/s) for both (a) and (b).

distributed along the vertical direction in the annulus. Instead, the width of the outflow regions (d_1) is significantly shorter than that of the inflow regions (d_2). Correspondingly, the mean outflow velocity is higher than the inflow velocity, as can be seen from Figure 2a. The ratio of d_2 to d_1 is 1.65, higher than the value of 1.3 at Re=124 reported by Wereley and Lueptow (1998). This can be explained by their statement that the differences between the inflow and outflow radial velocities are less distinct with a smaller Reynolds number.

Figure 2b shows the calculated velocity field from Fluent simulations. It can be seen that the simulation results agree qualitatively well with the experimental data by exhibiting all the features observed above. For example, there are also six vortices of similar shape, and the vortex centers from our simulation also exhibit an inclination to the outer cylinder although it is less significant than in the experimental results. The calculated ratio of d_2 to d_1 is 1.49, a little bit smaller than the experimental value. More quantitative results about the velocity are shown in the following section.

3.2 Axial velocity in the gap

By tracking the axial velocity from C to C´ along the dashed line shown in Figure 2b, we can examine the velocity profile at various rotation speeds, as shown in Figure 3a. The axial velocity at both the inner and outer cylinder wall equals to zero as a result of the no-slip boundary conditions adopted there. At lower rotation speeds, the axial velocity tends to be symmetric around ξ=0.5. However, this symmetry is less significant with increasing rotation speeds, corresponding to a more significant displacement of vortex centers towards the outer cylinder. Also, the maxima on the curves of V_{axial} versus ξ shift to the inner cylinder with increasing rotation speeds while the minima show the opposite trend.

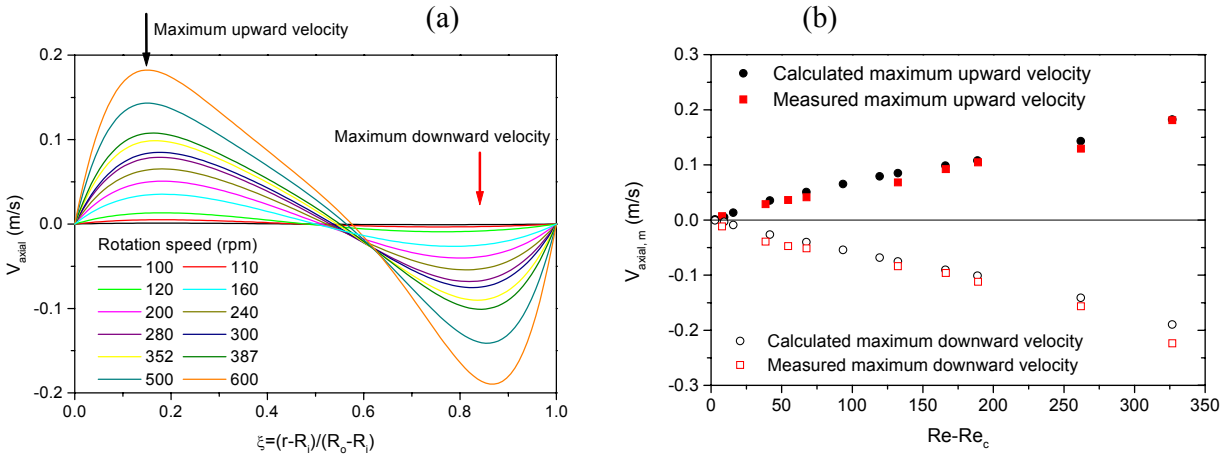

Figure 3: (a) Calculated axial velocity profile along the radial direction. (b) Calculated and measured maximum axial velocity at various reduced Reynolds numbers.

As shown in Figure 3b, the calculated and measured maximum axial velocities are consistent with each other. In the range of our operating conditions, the absolute value of V_{axial} is found to be always less than 20% of the azimuthal velocity of the inner cylinder, showing that the intensity of the secondary flow (Taylor vortex flow) is significantly lower than the primary flow. Surprisingly, the maximum axial velocity (both upward and

downward) increases almost linearly with the increasing reduced Reynolds number. This is different from Davey's prediction for the axial (or radial) velocity in an infinitely long liquid column (Davey, 1962). Two reasons may be attributed to this difference: (1) Davey's expansion is most appropriate very near the transition to Taylor vortex flow and (2) The axial velocities in the short column are significantly influenced by the Ekmon vortices.

3.3 Effects of top and bottom liquid layers

In the present study, the inner cylinder is immerged in the working liquid. The liquid layers above and below the inner cylinder, as well as the liquid in the annulus, compose a continuous flow field. Thus, the thickness of the top and bottom layers can influence the Taylor vortex formation in the gap.

Figure 4 shows the Taylor vortex structures in the presence of a top layer of different thicknesses. It can be seen that, the number of vortices (excluding the end vortex

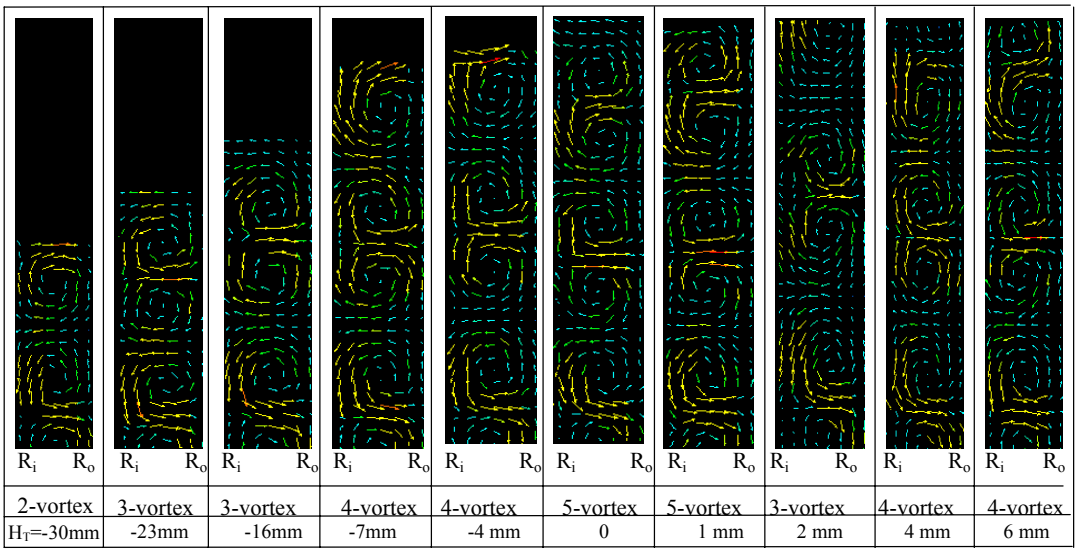

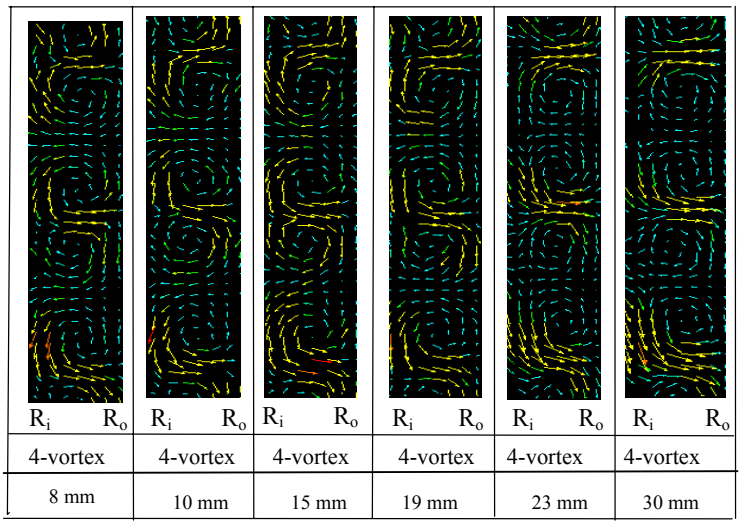

Figure 4: Effects of top layer thickness on Taylor vortex formation in the annulus. *Re*=130, H_B=72mm. The number labeled below each panel is H_T.

at the bottom) gradually increases from two to five with the increasing liquid height in the annulus until the mineral oil surface is on par with the top of the rotating inner cylinder. This can be explained by that the increase in annulus length allows more Taylor vortices to be formed. As H_T continues to increase, some anomalous phenomenon is observed. Five vortices appear when H_T equals to 0 and 1mm, while only three vortices (excluding the end vortex at the top) can be observed with a layer thickness of 2mm. When H_T increases to 4mm, there are four complete vortices in the annulus. Any further increase of the top layer thickness no longer changes the number, position and shape of the vortices.

An examination on the vortex flow direction may offer us a better understanding of the boundaries. When the liquid surface is lower than the top of the inner cylinder (H_T<0), it is a truly “free” end such that the flow at the surface can be either inward or outward depending on the length of the liquid column, and the number of vortices can be either even or odd. However, when H_T >>0, the end vortex near the top of the inner cylinder is suppressed by a thick liquid layer at the top, which functions as a “fixed” end similar to the thick liquid layer below the inner cylinder (H_B=72mm). As a result, the flow at the top end also points outwards. In this case, the two boundaries at the top and bottom show some kind of “symmetry”. This may explain why we observe an almost symmetric vortex structure with H_T=30mm, where two pairs of vortices locating at the center and one outflowing vortex at each end.

During the above change of top layer thickness, the end vortex at the bottom almost keeps unchanged, showing a very stable flow structure below the inner cylinder. Such stability can also be achieved at the top by increasing the top layer to a high enough thickness (H_T should be at least 66mm).

In order to observe a significant influence of the bottom liquid layer, we purposely establish a relatively “free” boundary at the top by setting H_T=0, with the results shown in Figure 5. It can be seen that, when H_B reduces from 73 to 39mm, the whole flow field in the annulus almost keeps unchanged, with five full vortices and an incomplete end vortex at the bottom. As H_B continues to decrease, the number of vortices starts to vary, and the rotation direction of the top end vortex may change from anti-clockwise to clockwise. A further decrease in H_B to below 24mm can push the bottom end vortex to shift upwards along the annulus, as shown by the red arrow. When there is only 1mm liquid layer left, the bottom end vortex can almost be fully observed from the annulus.

From the above analysis we can see that, when H_T>6mm and H_B>39mm, the vortex structure will no longer be influenced by the variation of liquid layer thickness at either end. In the application of a Taylor vortex unit (reactor, exactor, filter, etc.), the column length is invariably finite, and boundary effects should be taken into consideration. If a “free” end is involved, one possible approach is to “stabilize” the boundary, for example, by introducing a thick liquid layer at that end. As a result, the Taylor vortex flow may not easily influenced by the oscillation of some parameters, and the operation can be rather robust.

4 Conclusions

With the help of PIV, we have determined the Taylor vortex flow field (including vortex number, position, shape and velocity profile) formed in a short column with

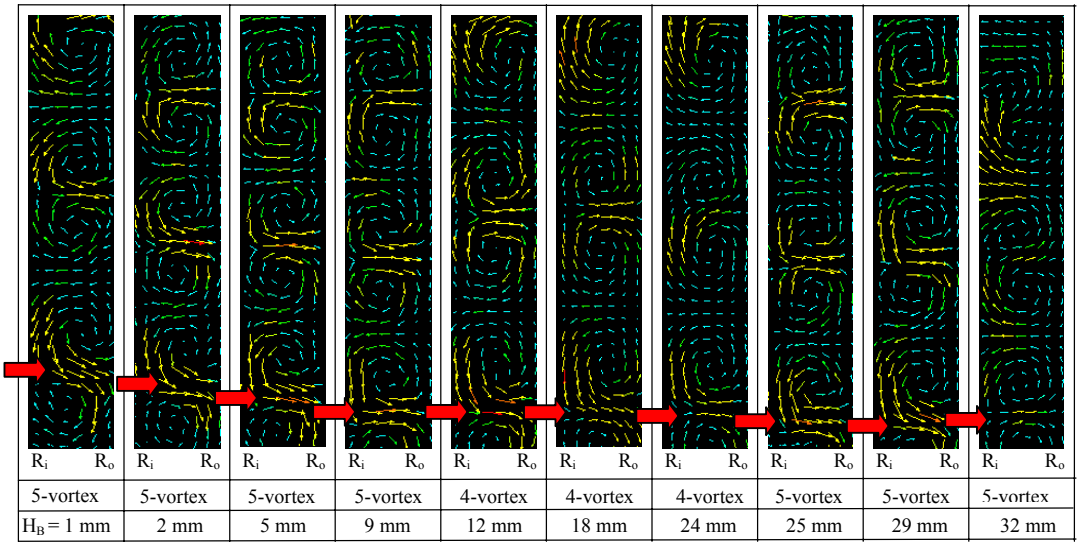

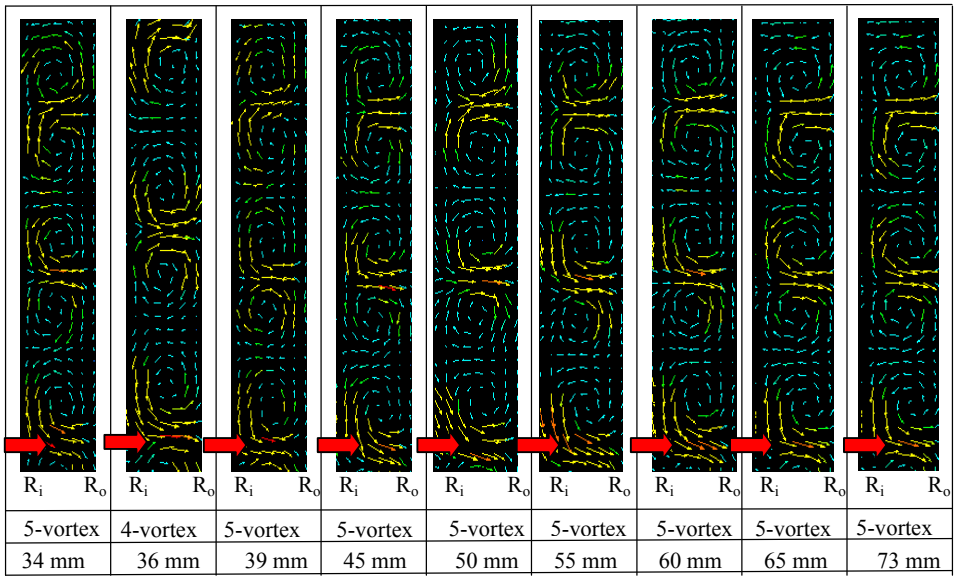

Figure 5: Effects of bottom layer thickness on Taylor vortex formation in the annulus. *Re*=130, H_T=0. The number labeled below each panel is H_B.

significant boundary effects. The calculation results from Fluent simulation match well with the experimental observations. The boundaries at the top and the bottom can significantly affect the vortex formation in the annulus. More quantitative results on this system are to come in the future from both experiments and CFD simulation.

Acknowledgements

This project is supported by National University of Singapore, Singapore-MIT Alliance and Massachusetts Institute of Technology.

References

Baier G. and Graham M. D. “Two-fluid Taylor-Couette flow with countercurrent axial flow: Linear theory for immiscible liquids between corotating cylinders”, *Phys. Fluids*, 12(2):294-303, 2000.

Baier G., Graham M. D. and Lightfoot E. N. “Mass transport in a novel two-fluid Taylor vortex exactor”, *AIChE J.*, 46 (12): 2395-2407, 2000.

Benjamin T. B. “Bifurcation phenomena in steady flows of a viscous fluid. I. Theory”, *Proc. R. Soc. London Ser. A,* 359:1-26, 1978.

Bielek C. A. and Koschmieder E. L. “Taylor vortices in short fluid columns with large aspect ratio”, *Phys. Fluids A*, 2(9):1557-1563, 1990.

Cole J. A. “Taylor-vortex instability and annulus-length effects”, *J. Fluid Mech.*, 75:1-15, 1976.

Czarny O., Serre E., Bontoux P. and Lueptow R. M. “Spiral and wavy vortex flows in short counter-rotating Taylor-Couette cells”, *Theoret. Comput. Fluid Dynamics*, 16:5-15, 2002.

Davey A. “The growth of Taylor vortices in flow between rotating cylinders”, *J. Fluid Mech.*, 14:336-368, 1962

Drozdov S., Rafique M. and Skali-Lami S. “An asymmetrical periodic vertical structures and appearance of the self induced pressure gradient in the modified Taylor flow”, *Theoret. Comput. Fluid Dynamics*, 18:137-150, 2004.

Dutta P. K. and Ray A. K. “Experimental investigation of Taylor vortex photcatalytic reactor for water purification”, *Chem. Eng. Sci.*, 59:5249-5259, 2004.

Edwards W.S., Beane S. R. and Varma S. “Onset of wavy vortices in the finite-length Couette-Taylor problem”, *Phys. Fluids A*, **3**:1510-1518, 1991.

Koga J. K. and Koschmieder E. L. “Taylor vortices in short fluid columns”, *Phys. Fluids A* 1(9):1475-1478, 1989.

Marchisio D. L. and Barresi A. A. “CFD simulation of mixing and reaction: the relevance of the micro-mixing model”, *Chem. Eng. Sci.*, 58:3579-3587, 2003.

Marchisio D. L., Barresi A. A. and Fox R. O. “Simulation of turbulent precipitation in a semi-batch Taylor-Couette reactor using CFD”, *AIChE J.*, 47(3):664-676, 2001.

Painter B. D. and Behringer R. P. “Effects of spatial disorder on the transition to Taylor vortex flow”, *Europhysics Lett.*, 44(5):599-605, 1998.

Smieszek M. and Egbers C. “Flow structures and stability in Newtonian and non-Newtonian Taylor-Couette flow”, *J. Phys. Conf. Ser.*, 14:72-77, 2005.

Wang L., Marchisio D. L., Vigil R. D. and Fox R. O. “CFD simulation of aggregation and breakage processes in laminar Taylor-Couette flow”, *J. Colloid Interface Sci.*, 282:380-396, 2005.

Wang L., Vigil R. D. and Fox R. O. “CFD simulation of shear-induced aggregation and breakage in turbulent Taylor-Couette flow”, *J. Colloid Interface Sci.*, 285:167-178, 2005.

Wereley S. T. and Lueptow R. M. “Spatio-temporal character of non-wavy and wavy Taylor-Couette flow”, *J. Fluid Mech.*, 364:59-80, 1998.

Wereley S. T., Akonur A. and Lueptow R. M. “Particle-fluid velocities and fouling in rotating filtration of a suspension”, *J. Membrane Sci.*, 209: 469-484, 2002.

Yim S. S. S., Lo M. Y. A., Titchener-Hooker N. and Ayazi Shamlou P. “The dependence of residence time distribution on flow in co-axial cylinder devices”, *Bioprocess Eng*. **19**: 221-227, 1998.

Zhu X. and Vigil R. D. “Banded liquid-liquid Taylor-Couette-Poiseuille flow”, *AIChE J.*, 47:1932-1940, 2001.